British Journal of Cancer Research
2019; 2(4): 314 - 319. doi: 10.31488/bjcr.137

Research article

Thapsigargin induced Apoptosis Occurs with a Delayed DNA Damage Response

A Vossenkamper[1], G Warnes[*2],

1. Centre for Immunobiology, The Blizard Institute, Barts and The London School of Medicine and Dentistry, Queen Mary London University, 4 Newark Street, London

2. Flow Cytometry Core Facility, The Blizard Institute, Barts and The London School of Medicine and Dentistry, Queen Mary London University, 4 Newark Street, London

[*]Corresponding author: Flow Cytometry Core Facility, The Blizard Institute, Barts and The London School of Medicine and Dentistry, Queen Mary London University, 4 Newark Street, London E1 2AT, Tel: 44(0)20-7882-2402; E-mail:g.warnes@qmul.ac.uk

Received: July 02, 2019; Accepted: August 14, 2019; Published: August 16, 2019

Abstract

The intracellular immunophenotyping of antigens involved in Regulated Cell Death (RCD) has allowed the detection flow cytometrically of several of these processes simultaneously. it permits the detailed analysis of the degree of classic early apoptosis (Zombie^{-ve}/Caspase- 3^{+ve}/RIP3^{-ve}), RIP1 dependent apoptosis (Caspase-3+ve/RIP3+ve), late apoptosis (Zombie- ve/Caspase-3^{+ve}/RIP3^{-ve}), necroptosis or resting cells (RIP3$^{Hi+ve/+ve}$/Caspase-3^{-ve}), parthanatos or hyper-activation of PARP (H2AX^{+ve}/PARP^{+ve}/Caspase-3$^{\pm ve}$), DNA Damage Response (DDR) and cleaved PARP within live and dead cells. The sarco/endoplasmic reticulum inhibitor thapsigarin (Tg) induced apoptosis which was reduced by zVAD, while the observed oncosis was unaffected by necrostatin-1. Tg up-regulated parthanatos in live and dead resting Jurkat cells (Zombie$^{\pm ve}$/-Caspase-3^{-ve}/RIP3$^{\pm ve}$). Tg treatment lead to reduced DDR in live resting cells and live RIP1-dependent apoptotic cells. All dead cell phenotypes showed an increased incidence of DDR and a decrease of cleaved PARP. zVAD blockade of Tg decreased DDR in dead apoptotic dead cell populations and increased parthanatos in dead resting cells. While necrostatin-1 blockade increased DDR in live and dead resting cells and decreased cleaved PARP in all live cell phenotypes. Necrostatin-1 blockade of Tg also resulted in increased levels of parthanatos in dead resting oncotic cells. In conclusion, we demonstrate here the effects of the drug Tg on various cell death pathways by employing a flow cytometric assay that allows researchers to perform a more in-depth gain more screen of the mode of action of drugs. This approach may be useful in the targeting of drugs in the treatment of cancer.

Keywords: thapsigargin, apoptosis, DNA damage response, parthanatos, flow cytometry

Introduction

The three types of cell death have been placed into three named major divisions which currently include Accidental Cell Death (ACD), Programmed Cell Death (PCD) and Regulated Cell Death (RCD). Broadly this included firstly oncosis, secondly homeostatic apoptosis and thirdly programmed apoptosis and necrosis and includes macro-micro-autophagy [1-4]. Cell death research has been achieved by the excellent use of Western Blot and fluorescent microscopy over many decades identifying more forms of cell death from initial identification of apoptosis, autophagy and necrosis as the three broad forms of regulated cell death [1-4]. Flow cytometry with its multi-parameter capability has been under-employed since it was being used to mainly study apoptosis [5,6]. The recent development of a multi-parameter immunophenotyping flow cytometric based assay identifying eight forms of RCD and two of ACD each divided into numerous sub-populations has highlighted the complexity of the links between all of these forms of cell death [7-9]. This assay also showed that dead cells have a similar profile no matter what form of cell death or drug was employed. This highlights a potential significant issue with the use of Western Blot technology which does not consider the ratio of live to dead cells within a cell sample which can cause a biasing of the observed result [7-9]. Also, there are still problems of obtaining only one result from one sample when employing the Western Blot approach when clearly there are multiple forms of cell death occurring simultaneously [7-9]. The flow cytometry assay has been used to identify necroptosis, apoptotic and riptosome expressing cells (RIP1-dependent apoptosis) based upon cell viability/RIP3/-Caspase-3 phenotyping. It was further sub-divided into defined populations bearing the biological markers for DNA damage H2AX and cleaved PARP. These extra markers allow the identification of cells undergoing the DNA Damage Response (DDR,

H2AX+ve/PARP-ve), cleaved PARP as a result of Caspase-3 dependent apoptosis ($H2AX^{-ve}/PARP^{+ve}$) and hyper-activation of PARP ($H2AX^{+ve}/PARP^{+ve}$) indicating parthanatos in cells not expressing Caspase-3 [10-12].

Autophagy has been shown to reduce the level of DNA Damage within live resting Jurkat cells ($RIP3^{+ve}$/Caspase-3^{-ve}) and increased DDR levels in resting dead Jurkat cells [9,13]. Oncosis has been shown to consist of two main dead populations based upon cell viability/RIP3/Caspase-3 phenotyping which were also shown to express H2AX and PARP allowing the identification of DDR (H2AX), cleaved PARP, hyper-activation of PARP in apoptotic cells or parthanatos in Caspase-3 negative cells [9,11,14-16].

This flow cytometric approach to simultaneously measure multiple forms of cell death has been useful in studying the mode of action of cell death inducing drugs. Thapsigargin (Tg) is a sesquiterpene lactone [17] which has previously been reported to induce numerous affects upon different cell types including cell cycle arrest [18,19], apoptosis [20-24], endoplasmic reticulum (ER) stress [19,20,25,26], parthanatos [12,15,25], initiation and blockade of autophagic flux at the lysosomal fusion step (19) and induction of regulated necrosis via it's affects upon mitochondrial function [14,15,25]. We set out to investigate Tg's effects using this assay to gain more insight into the complexity of the resulting multiple forms of RCD which can be simultaneously identified in Jurkat cells which are commonly employed in cell death studies. Additionally, we employed blockers of caspase and kinase activity, zVAD and necrostatin-1 to block apoptosis and necroptosis respectively. They may also modify the degree of DDR, cleaved PARP, hyper-activation of PARP or parthanatos induced by the action of Tg in the multiple regulated cell death phenotypes which may give an insight into RCD and ACD interconnectivity. This flow cytometric assay therefore can be used as a screening tool to serve in the in-depth analysis of the mechanisms of action of new anti-cancer therapeutic drugs.

Materials and Methods

Induction of oncosis and apoptosis

Jurkat cells (human acute T cell leukaemia cell line) were grown in RPMI 1640 medium with 10% FBS and penicillin/streptomycin (Invitrogen, UK) at 37°C and 5% CO2 and either left untreated or treated with 7 µM thapsigargin (Tg, Enzo Life Sciences, UK) for 24 h. Cells were also pre-treated with the pan-caspase blocker zVAD (20 µM, Enzo Life Sciences, USA) and/or the necroptosis blocker necrostatin-1 (60 µM Cambridge Bioscience, UK) for 2 h before induction of oncosis with 7 µM thapsigargin for 24 h.

Flow cytometric assay

Harvested cells were labelled with fixable live dead stain, Zombie NIR (Near Infra-Red) (BioLegend, UK) at RT for 15 mins. Washed cell pellets were sequentially fixed in Solution A (CalTag, UK) then 0.25% Triton X-100 (Sigma, UK) for 15 min each at RT. Jurkat cells (1 $x10^6$) were incubated for 20 min at RT with 2 µl of anti-RIP3-PE (clone B-2, Cat. No. sc-374639, Santa Cruz, USA), cleaved anti-PARP-PE-CF-595 (clone F21-852, Becton Dickinson, USA), anti-H2AX-PE-Cy7 (clone F21-852, Becton Dickinson, USA), anti-H2AX-PE-Cy7 (clone 2F3, BioLegend, UK) and anti-active caspase-3-BV650 (clone C92- 605, Becton Dickinson, USA) for 20 min at RT. Washed cells were resuspended in 400 µl PBS and analysed on a ACEA Bioscience Novocyte 3000 flow cytometer (100,000 events). Zombie NIR was excited by the 633 nm laser and collected at 780/60 nm detector. Caspase-3-BV650 was excited by the 405 nm laser and collected at 675/30 nm. RIP3-PE, cleaved PARP-PE- CF-595, H2AX-PE-Cy7 were excited by the 488 nm laser and collected at 572/28, 615/20, 780/60 nm respectively. Single colour controls were employed to determine the colour compensation using the pre-set voltages on the instrument using Novo Express software (ver 1.2.5, ACEA Biosciences, USA). Cells were gated on FSC vs SSC removing the small debris near the origin with single cells being gated on a FSC-A vs FSC-H dot-plot. Cells were then gated on a dot-plot of Caspase-3-BV650 vs Zombie NIR with a quadrant placed marking off live cells in the double negative quadrant (lower left), with Caspase-3-$BV650^{+ve}$/Zombie NIR^{-ve} (lower right) indicating early apoptotic cells and lastly with Caspase-3-$BV650^{+ve}$/Zombie NIR^{+ve} and Caspase-3-$BV650^{-ve}$/-Zombie NIR^{+ve} upper quadrants indicating late dead apoptotic and necrotic cells, respectively (Figure 1A). Live (including early apoptotic) and dead cells were gated separately and analysed in RIP3 vs Caspase-3 dot-plots with $RIP3^{+ve}$/-Caspase-3^{-ve} indicating normal resting cells or necroptosis when RIP3 Median Fluorescence Intensity (MFI) was up-regulated (Figure 1B, C). $RIP3^{-ve}$/Caspase-3^{+ve} cells indicate those that have undergone apoptosis. Double positive events indicate cells of the RIP1-dependent apoptosis phenotype in live and dead cells (Figure 1B, C). This is an assumed observation, as RIP3 is associated with RIP1 in the formation of the necrosome [27] (RIP1 and RIP3 was observed to be present in PBMNC, data not shown [7]). Double negative cells and all other phenotypes were further analysed for H2AX and PARP expression (Figure 1B, C). The following populations were identified: DDR was identified as $H2AX^{+ve}/PARP^{-ve}$ events, hyper-activation of PARP or parthanatos as $H2AX^{+ve}/PARP^{+ve}$, cleaved PARP by caspase-3 dependent apoptosis as $H2AX^{-ve}/PARP^{+ve}$ and quadruple negative (QN, $H2AX^{-ve}/PARP^{-ve}$) as shown in Figure 1D, E.

Statistics

All experiments n=3, with results expressed as mean±SEM for percentage positive. Student t tests were performed in Graph Pad software Inc., USA with P = >0.05 not considered significant (NS), P = <0.05*, P = <0.01**, P= <0.001*** when treated cells were compared to untreated.

Results

Tg induction of cell death with caspase and RIP1 blockade

Tg induced oncosis (Zombie^{+ve}/Caspase-3^{-ve}), early (Zombie^{-ve}/Caspase-3^{+ve}) and late apoptosis (Zombie^{+ve}/Caspase-3^{+ve}) with zVAD reducing early and late apoptosis (Figure 2 A, B, C, Figure 3A-F). Necrostatin-1 blockade of Tg reduced the degree of overall cell death with a higher proportion of live cells being present compared to that with Tg alone (Figure 2D, Figure 3G, H). Dual blockade of Tg reduced early and late apoptosis as

observed with zVAD blockade alone (Figure 2E, Figure 3I, J). Tg also increased the incidence of live cells that were DN for RIP3 and Caspase-3, 26% compared to 10% in untreated cells (Figure 3A, C). Blockade of Tg with zVAD or Nec-1 increased this live DN population to 35-40%, with dual blockade inducing a summative affect with 60% being live DN indicating that cells are no longer in a resting state (Figure 3E, G, I). Whereas dead cells only showed this effect of increasing DN population after blockade of Tg with zVAD (67%) and dual blockade (63%, Figure 3F, H, J).

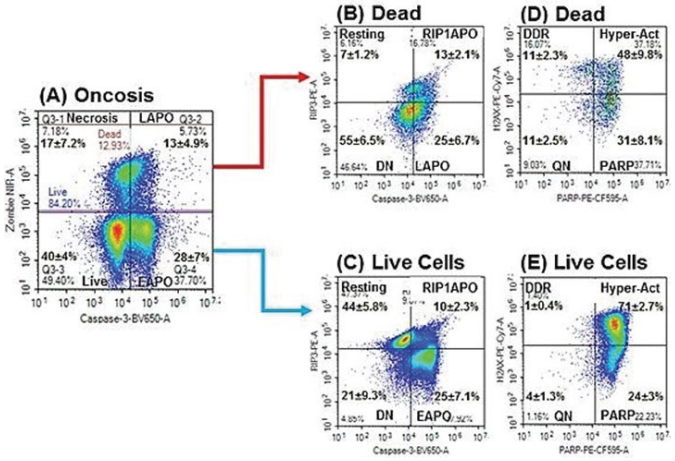

Figure 1. Gating strategy of immunophenotyping of RCD. Live (including early apoptotic, EAPO) and dead including late apoptotic (LAPO) and necrotic cells were gated from a Zombie NIR vs. Caspase-3-BV650 dot-plot (A). Live and dead necroptotic cells were defined as Caspase-3^{-ve}/RIP3high^{+ve}, early or late apoptotic (Caspase-3^{+ve}/RIP3^{-ve}), RIP1-dependent apoptotic (RIP1-APO, Caspase-3^{+ve}/RIP3^{+ve}) and double negative (DN, Caspase-3^{-ve}/RIP3^{-ve}) (B, C). Then each of these live and dead cell populations were then gated on a H2AX vs. PARP dot-plots to show the incidence of DDR (H2AX^{+ve}/PARP^{-ve}), hyper-activation of PARP/parthanatos (H2AX^{+ve}/PARP^{+ve}), cleaved PARP (H2AX^{-ve}/PARP^{+ve}) and quadruple negative (QN, H2AX^{-ve}/PARP^{-ve}), (D, E).

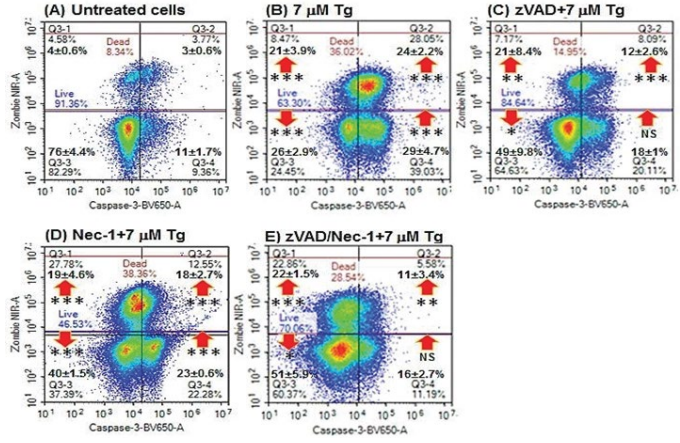

Figure 2. Cell death and caspase-3 activation assay. After 24 h treatment Jurkat cells were incubated with live-fix dye Zombie NIR, fixed, permeabilised and incubated with anti-active caspase-3-BV650 according to the Materials and Methods and 100,000 cells were analysed flow cytometrically. Jurkat cells were untreated (A), treated with 7 µM Tg for 24 h (B), pre- treated with 20 µM zVAD for 2 h then treated with 7µM Tg for 24 h (C), pre-treated with 60 M necrostatin-1 (Nec-1) for 2 h then treated with 7 µM Tg for 24 h (D), pre-treated with 20 µM zVAD and 60 µM necrostatin-1 (Nec-1) for 2 h then treated with 7 µM Tg for 24 h (E), n=3, student t test NS (not significant), P<0.05*, P<0.01**, P<0.001***, with arrows indicating change compared to untreated cells.

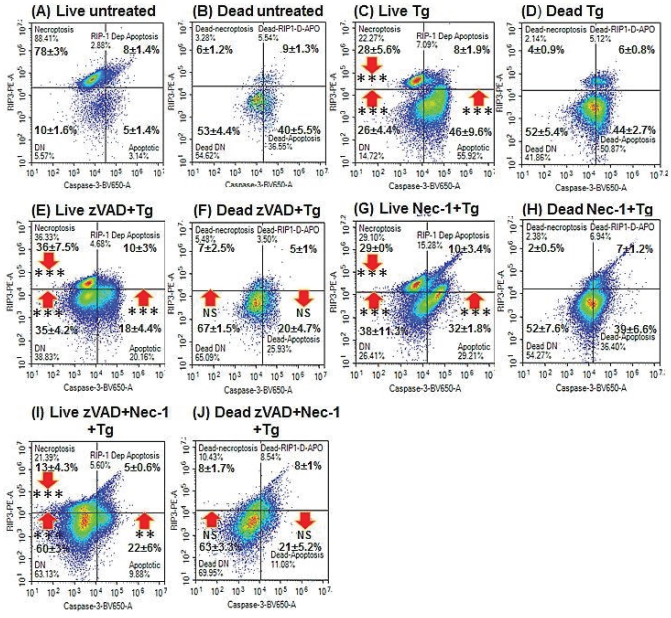

Figure 3. RIP3 and caspase-3 activation assay. After 24 h treatment Jurkat cells were incubated with live-fix dye, Zombie NIR, fixed, permeabilised and incubated with anti-active caspase-3-BV650 and RIP3-PE according to the Materials and Methods and 100,000 cells were analysed flow cytometrically. After gating on live and dead cells from a Zombie NIR vs Caspase3-BV650 dot-plot untreated live (A) and dead (B) Jurkat cells were analysed on a RIP3-PE vs Caspase-3-BV650 dot-plot with resting phenotype or RIP3^{+ve}/-Caspase-3^{-ve}. The apoptosis phenotype or RIP3^{-ve}/Caspase-3^{+ve}, RIP1-dependent apoptosis or RIP3^{+ve}/Caspase-3^{+ve} and double negative indicated by RIP3^{-ve}/Caspase-3^{-ve}. Live and dead cells treated with 7 µM Tg for 24 h (C), (D), pre-treated with 20 µM zVAD for 2 h then treated with 7 µM Tg for 24 h (E), (F), pre-treated with 60 µM Nec-1 for 2 h then treated with 7 µM Tg for 24 h (G), (H), pre-treated with 20 µM zVAD and 60 µM Nec-1 for 2 h then treated with 7 µM Tg for 24 h (I), (J). n=3, student t test NS (not significant), P<0.05*, P<0.01**, P<0.001***, with arrows indicating change compared to untreated cells.

Modulation of DDR, hyper-activation of PARP/parthanatos and cleaved PARP by Tg in live cells

The different untreated live cell phenotypes showed very different profiles for the incidence of DDR, hyper-activation of PARP/parthanatos and cleaved PARP. Resting live cells (Zombie^{-ve}/RIP3^{+ve}/Caspase-3-ve) showed a high degree of DDR (37%) which was reduced by treatment with Tg (10%, Figure 4A, B). Untreated early apoptotic cells showed a high level of cleaved PARP (66%) which was reduced by Tg (56%) and a moderate level of H2AX hyper-activation of PARP (21%) which was increased by Tg (38%, Figure 4F, G). Untreated live RIP1- dependent apoptotic cells like resting cells showed a high degree of DDR (31%) which was again reduced by Tg (2%, Figure 4K, L). Tg also increased levels of cleaved PARP (26%) and hyper-activation of PARP in live RIP1-dependent apoptotic cells (65%, Figure 4K, L).

Lastly, live untreated DN cells showed a high degree of cleaved PARP which was unaffected by Tg, although this population increased levels of DDR (6%) and parthanatos (12%, Figure 4P, Q).

Modulation of DDR, hyper-activation of PARP and parthanatos by Tg in dead cells

The phenotypes of dead untreated cells showed very different profiles for the incidence of DDR, hyper-activation of PARP/ parthanatos and cleaved PARP compared to live cells. Resting dead cells (Zombie^{+ve}/RIP3^{+ve}/Caspase-3^{-ve}) showed moderate levels of DDR (21%), cleaved PARP (19%) and parthanatos (14%) all of which were unaffected by Tg except with a reduction in cleaved PARP (9%, Figure 5A, B).

Untreated late apoptotic cells and early apoptotic cells showed a high degree of cleaved PARP (56%) which was reduced by Tg (24%) and a moderate level of hyper-activation of PARP (28%) which was increased by Tg as was DDR respectively (41%, 30%, Figure 5F, G). Dead untreated RIP1-dependent apoptotic cells (unlike live cells) showed little DDR and more cleaved PARP (31%) which was decreased by Tg (22%) and hyper-activation of PARP (45%) which was increased by Tg (65%, Figure 5K, L). The dead untreated oncotic DN cells showed a low degree of cleaved PARP (18%) with a high degree of QN cells (64%) very much like the live DN cells (Figure 5P). Tg caused a reduction in the QN population of the dead oncotic phenotype (44%) with an increase in DDR (31%) and parthanatos (17%) compared to untreated cells (6%, Figure 5Q).

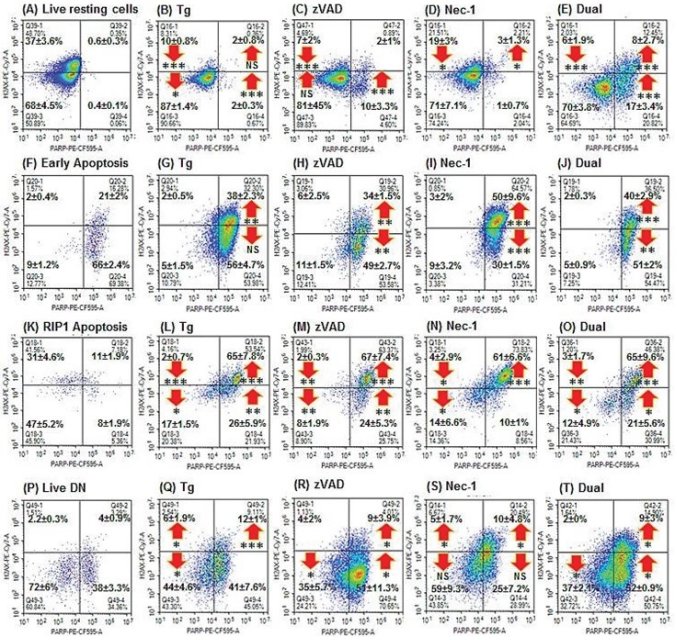

Figure 4. Live cell hyper-activation of PARP/parthanatos cleaved PARP and DDR assay. Jurkat cell were left untreated, treated with 7 µM Tg or pre-treated zVAD (20 µM) and or necrostatin-1 (Nec-1: 60M) for 2 h then incubated with 7 µM Tg for 24 h. After gating on live cells from a Zombie NIR vs. Caspase-3-BV650 dot-plot untreated or treated live and dead Jurkat cells were analysed on a RIP3-PE vs Caspase-3-BV650 dot-plot. From this plot live resting, early apoptotic, RIP1-dependent apoptotic and double negative (DN) populations were analysed for H2AX and PARP. The phenotypes for DDR (H2AX-$^{+ve}$/PARP^{-ve}), hyper-activation of PARP/parthanatos (H2AX-$^{+ve}$/PARP^{+ve}), cleaved PARP (H2AX^{-ve}/PARP^{+ve}) and quadruple negative (QN, H2AX^{-ve}/PARP^{-ve}) were then analysed. n=3, student t test NS (not significant), P<0.05*, P<0.01**, P<0.001*** compared to untreated cells.

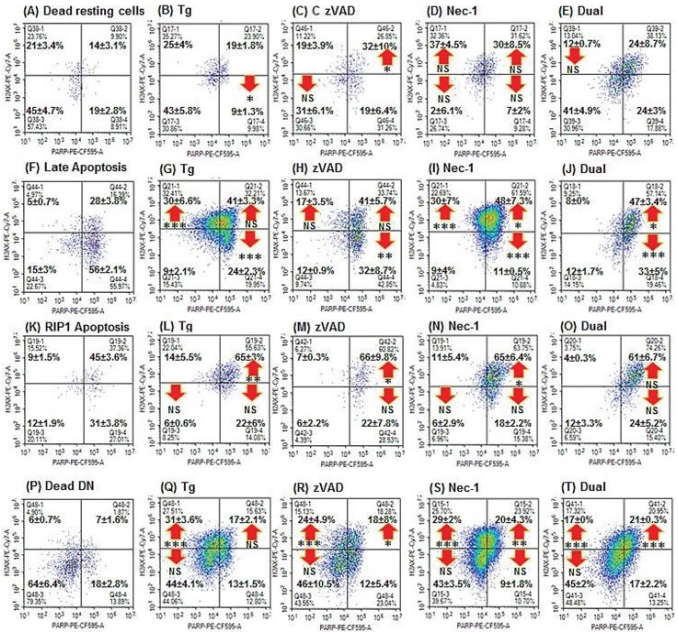

Figure 5. Dead cell hyper-activation of PARP/parthanatos, cleaved PARP and DDR assay. Jurkat cells were left untreated, treated with 7 µM Tg or pre-treated with zVAD (20 µM) and or necrostatin-1 (Nec-1; 60 µM) for 2 h then incubated with 7 µM Tg for 24 h. After gating on dead cells from a Zombie NIR vs. Caspase-3-BV650 dot-plot untreated or treated live and dead Jurkat cells were analysed on a RIP3-PE vs Caspase-3-BV650 dot-plot. From this plot dead resting, late apoptotic, RIP1-dependent apoptotic and double negative (DN) populations were analysed for H2AX and PARP. The phenotypes for DDR (H2AX-$^{+ve}$/PARP^{-ve}), hyper-activation of PARP/parthanatos (H2AX-$^{+ve}$/PARP^{+ve}), cleaved PARP (H2AX^{-ve}/PARP^{+ve}) and quadruple negative (QN, H2AX^{-ve}/PARP^{-ve}) were then analysed. n=3, student t test NS (not significant), P<0.05*, P<0.01**, P<0.001*** compared to untreated cells.

Modulation of DDR, hyper-activation of PARP/parthanatos and cleaved PARP by Tg and zVAD

Although zVAD reduced levels of early and late apoptosis induced by Tg, levels of DDR, hyper-activation of PARP/parthanatos and cleaved PARP were not significantly changed by zVAD in all live cell phenotypes compared to drug alone, except the increase in cleaved PARP in the live DN cell population (Figure 4C, H, M, R). While the dead cell phenotypes generated by Tg/zVAD treatment were only different to that observed with Tg in that dead resting oncotic cells showed increased parthanatos with a return of cleaved PARP back to levels observed in untreated cells (Figure 5A-C). Late apoptotic and RIP-dependent apoptotic cells showed reduced levels of DDR. Late apoptotic cells showed increased levels of cleaved PARP compared to drug treatment alone (Figure 5G, H, L, M).

Modulation of DDR, hyper-activation of PARP/parthanatos and cleaved PARP by Tg and Necrostatin-1

Although Nec-1 blockade of Tg only resulted in fewer dead cells (40%) compared to Tg (26%), the resting live cell phenotypes showed less DDR (19%) than untreated cells (37%) but more than Tg alone (10%, Figure 4A, B, D). While early apoptotic and live DN populations showed less cleaved PARP (Figure 4 A, D, F, I, P, S). Also all the live cell phenotypes after Tg/Nec-1 treatment showed increased parthanatos/hyper-activation of PARP respectively (Figure 4 A, D, F, I, K, N, P, S).

Whereas the dead cell phenotypes also all showed less cleaved PARP than that observed with Tg (Figure 5 A, D, F, I, K, N, P, S). Although all dead phenotypes showed the increased parthanatos/hyper-activation of PARP and DDR above that of observed with untreated cells (Figure 5 A, B, D, F, I, K, N, P, S). Modulation of DDR, hyper-activation of PARP and parthanatos by Tg, zVAD and Necrostatin-1

Although dual blockade of Tg only reduced the degree of early and late apoptosis in a similar manner to that of zVAD blockade the incidence of live and dead DN cells was >60% and the highest level shown in this study (Figure 2E, Figure 3I, J). The live resting and DN cell phenotypes showed decreased DDR with increased levels of cleaved PARP and parthanatos similar to that observed in zVAD/Tg treated live DN cells (Figure 4P, R, T). Early apoptotic cells treated with Tg/zVAD/Nec-1 as with Tg alone showed less cleaved PARP and RIP1- dependent apoptotic cells showed less DDR (Figure 4A, E, F, J, K, O, P, T). After dual blockade of Tg all dead cell phenotypes showed reduced levels of DDR compared to Tg and individual blockade treatments respectively (Figure 5).

Discussion

The development of a polychromatic flow cytometric immunophenotyping assay for measuring multiple forms of regulated cell death within a single sample has allowed the possibility of determining the degree of changes in a broader range of cell death parameters effected by drugs than ever before. Tg is a drug known to induce ER stress [19,20,25,26], apoptosis [20,22-24] and incomplete autophagy [19]. The simple flow cytometry assay employed here demonstrates the mode of action of Tg by revealing a number of effects it has upon cells [7-9]. Multiple phenotypes of cells were identified within the Jurkat population. These included live and dead (oncotic) resting cells, early and late apoptotic, RIP1-dependent apoptotic as well as live DN ($RIP3^{-ve}$/$Caspase\text{-}3^{-ve}$) and dead oncotic DN cells [9]. Tg induced apoptosis which was reduced by zVAD (pan-caspase blocker), while necrostatin-1 did not affect the degree (20%) of necrotic Jurkat cells although the incidence of live cells was increased [25,28]. Interestingly Tg also induced necrosis or oncosis which was shown not to be necroptosis, as determined in this assay by the lack of RIP3 up-regulation [7- 9,12,14,15,25].

However Tg also showed a range of affects upon the different cell phenotypes described in that the incidence of H2AX, cleaved PARP and hyper-activation of PARP or parthanatos (double positive) varied in each population and whether the cells were alive or dead. Tg caused a reduction in the degree of live cell DDR in live resting and RIP1-dependent apoptotic cells (with a marginal increase in DDR in live DN cells), which perhaps is related to Tg's ability to initiate autophagy which is known to reduce the degree of DDR [9,13,29]. This decrease in DNA repair in live cells is then mirrored by an increase in the DDR in all dead cell phenotypes compared to untreated cultures of Jurkat cells [9]. All live and dead phenotypes showed an increase in parthanatos when active caspase-3 was not present ($H2AX^{+ve}$/$PARP^{+ve}$/$Caspase\text{-}3^{-ve}$) and hyper-activation of PARP when present ($H2AX^{+ve}$/$PARP^{+ve}$/$Caspase\text{-}3^{+ve}$) in tandem with lower levels of cleaved PARP except in live RIP1-dependent apoptotic and resting cells [10-12,25]. So Tg not only induced apoptosis and autophagy along with associated DNA repair mechanisms but also induced parthanatos in both DN cell populations (RIP3-ve/Caspase-3-ve) and increased hyper-activation of PARP in all apoptotic cell populations [25].

Blockade of Tg induced apoptosis by zVAD resulted in no changes in the live cell phenotypic expression of H2AX and PARP compared to that observed with drug treatment alone except the increase in cleaved PARP in the live DN population. Dead cells from such blockade showed increased parthanatos and cleaved PARP in resting oncotic cells (caspase- 3-ve) compared to Tg treatment. Late apoptotic cells showed increased cleaved PARP with reduced DDR in both types of dead apoptotic cells compared to Tg treatment. Thus zVAD blockade of Tg appears to stop not only apoptosis but the enhancement of DDR in dead cells as previously reported with autophagy initiator chloroquine [9], while parthanatos is increased in dead oncotic resting cells [25].

Necrostatin-1 blockade of Tg did not reduce necrosis but increased parthanatos (like zVAD blockade) in dead oncotic resting cells. The reduction in DDR induced by Tg was partially blocked by necrostatin-1 in the live and dead resting phenotypes. Hyper-activation of PARP was increased further in early apoptotic cells by Nec-1/Tg with a corresponding decrease in cleaved PARP in the early apoptotic cells, late apoptotic, live RIP1-dependent apoptotic and DN cells.

Dual blockade of Tg caused an enhancement of parthanatos and cleaved PARP in live resting cells compared to other treatments. While live DN cells showed higher levels of cleaved PARP compared to Tg treatment, dead cells showed an enhanced decrease of DDR in dead oncotic resting and DN cells with dual blockade of Tg. Increased levels of cleaved PARP were observed in dead oncotic resting and late apoptotic cells with dual blockade of Tg compared to Tg alone.

This polychromatic flow cytometric assay showed that Tg and it's blockade by zVAD±Nec-1 changed the degree to which apoptosis and necrosis occurred but also the different levels of DDR, parthanatos/hyper-activation of PARP and cleaved PARP within four sub-populations of live and dead cells and the degree of modulation of these markers by these biological blocking agents. This approach to measuring the outcomes of drug treatments is a lot more refined than is currently available and thus its application in drug research screening will be extremely useful.

Abbreviations

ACD: accidental cell death; DDR: DNA Damage Response; DN: double negative; EAPO: early apoptosis; Tg: Thapsigargin; LAPO: late apoptosis; Nec-1: Necrostatin-1; PCD: programmed cell death; QN: quadruple negative; PARP: poly (ADP-ribose) polymerase; RCD: regulated cell death; RIP1APO: RIP1-dependent apoptosis

Acknowledgments

This research was supported in full from internal funding from Queen Mary University London.

Author Contributions

Conceived and designed experiments: GW: performed experiments GW, AV: Analysed the data: GW. Wrote and edited the paper: GW, AV.

Conflicts of interest statement

A. Vossenkamper received funding from GSK.

References

1. Galluzzi L, Aaronson SA, Abrams J, et al. Guidelines for the use and interpretation of assays for monitoring cell death in higher eukaryotes. Cell Death Differ. 2009;16:1093-107.
2. Galluzzi L, Bravo-San Pedro JM, Vitale I, et al. Essential versus accessory aspects of cell death: recommendations of the NCCD 2015. Cell Death Differ. 2015;22:58-73.
3. Galluzzi L, Vitale I, Abrams JM, et al. Molecular definitions of cell death subroutines: recommendations of the Nomenclature Committee on Cell Death 2012. Cell Death Differ. 2012;19:107-120.
4. Galluzzi L, Vitale I, Aaronson SA, et al. Molecular mechanisms of cell death: recommendations of the Nomenclature Committee on Cell Death 2018. Cell Death Differ. 2018;25:486-541.
5. Darzynkiewicz Z, Juan G, Li X, et al. Cytometry in Cell Necrobiology: Analysis of Apoptosis and Accidental Cell Death (Necrosis). Cytometry A. 1997;27:1-20.
6. E. Lugli, L Troaino, R Ferraresi, et al. Characterization of cells with different mitochondrial membrane poten- tial during apoptosis. Cytometry A. 2005;68A:28-35.
7. Lee HL, Pike R, Chong MHA, et al. Simultaneous flow cytometric immunophenotyping of necroptosis, apoptosis and RIP1-dependent apoptosis. Methods. 2018;134-135:56-66.
8. Vossenkamper A, Warnes G. A flow cytometric immunophenotyping approach to the detection of regulated cell death processes. J Immunol Sci. 2018;25:6-12.
9. Bergamaschi D, Vossenkamper A, Lee WYJ, et al. Simultaneous polychromatic flow cytometric detection of multiple forms of regulated cell death. Apoptosis. 2019;10.
10. Fatokun AA, Dawson VL, Dawson TM. Parthanatos: mitochondri-al-linked mechanisms and therapeutic opportunities. Brit J Pharmacol. 2014;171:2000-2016.
11. Boulares AH, Yakovlev AG, Ivanova V, et al. Role of Poly(ADP-ribose) Polymerase (PARP) Cleavage in Apoptosis. J Biol Chem. 199:22932-22940.
12. Berghe TV, Linkermann A, Jouan-Lanhouet S, et al. Regulated necrosis: the expanding network of non-apoptotic cell death pathways. Nat Rev Mol Cell Biol. 2014;15:135-47.
13. Czarny P, Pawlowska E, Bialkowska-Warzecha J, et al. Autophagy in DNA damage response. Int J Mol Sci. 2015;16:2641-62.
14. Zhu LP, Yu XD, Ling S, et al. Mitochondrial Ca(2+)homeostasis in the regulation of apoptotic and necrotic cell deaths. Cell Calcium. 2000;28:107-17.
15. Jiang HY, Yang Y, Zhang YY, et al. The dual role of poly(ADP-ribose) polymerase-1 in modulating parthanatos and autophagy under oxidative stress in rat cochlear marginal cells of the stria vascularis. Redox Biol. 2018;14:361-370.
16. Zhao N, Mao Y, Han G, et al. YM155, a survivin suppressant, triggers PARP-dependent cell death (parthanatos) and inhibits esophageal squamous-cell carcinoma xenografts in mice. Oncotarget. 2015;6:18445-18459.
17. Wictome M, Khan YM, East JM, et al. Binding of sesquiterpene lactone inhibitors to the Ca2+-ATPase. J Biochem. 1995;310:859-868.
18. Furuya Y, Lundmo P, Short AD, et al. The role of calcium, pH, and cell proliferation in the programmed (apoptotic) death of androgen-indepen-dent prostatic cancer cells induced by thapsigargin. Cancer Res.1994;54:6167-6175.
19. Ganley I, Wong P, Gammo N, et al. Distinct autophagosomal-lysosomal fusion mechanism revealed by thapsigargin-induced autophagy arrest. Mol Cell. 2011;42:731-43.
20. Kapuy O, Vinod PK, Banhegyi G. mTOR inhibition increases cell viabili-ty via autophagy induction during endoplasmic reticulum stress - An experimental and modeling study. FEBS Open Bio. 2014;4:704-13.
21. Lin X, Denmeade R, Cisek L, et al. Mechanism and role of growth arrest in programmed (Apoptotic) death of prostatic cancer cells induced by Thapsigargin. The Prostate. 1997;33:201-207.
22. Futami T, Miyagishi MKT. Identification of a networkiInvolved in thapsigargin- induced apoptosis using a library of Ssmall interfering RNA expression vectors. J Biol Chem. 2005;280:826-831.
23. Wang F, Liu DZ, Xu H, et al. Thapsigargin induces apoptosis by impairing cytoskeleton dynamics in human lung adenocarcinoma cells. Sci World J. 2014;2014:619050.
24. Tombal B, Weeraratna AT, Denmeade SR, et al. Thapsigargin induces a calmodulin/calcineurin-dependent apoptotic cascade responsible for the death of prostatic cancer cells. The Prostate. 2000;43:303-317.
25. Janssen K, Horn S, Niemann MT, et al. Inhibition of the ER Ca2+ pump forces multidrug-resistant cells deficient in Bak and Bax into necrosis. J Cell Sci. 2009;122:4481-91.
26. Mlynarczyk C, Fahraeus R. Endoplasmic reticulum stress sensitizes cells to DNA damage-induced apoptosis through p53-dependent suppression of p21(CDKN1A). Nat Commun. 2014;5:5067.
27. Conrad M, Angeli JP, Vandenabeele P, et al. Regulated necrosis: disease relevance and therapeutic opportunities. Nat Rev Drug Discov. 2016;15:348-66.
28. Popat A, Patel AA, Warnes G. A Flow Cytometric Study of ER Stress and Autophagy. Cytometry A 2018.
29. Potapova O, Basu S, Mercola D, et al. Protective role for c-Jun in the cellular response to DNA damage. J Biol Chem. 2001;276:28546-53.

To cite this article: A Vossenkamper, G Warnes. Thapsigargin induced Apoptosis Occurs with a Delayed DNA Damage Response. British Journal of Cancer Research. 2019: 2:4.